Magnetic Helicity Transport in the Quiet Sun

Brian Welsch & Dana Longcope

The flux of magnetic helicity through the solar photosphere has implications in diverse areas of current solar research, including solar dynamo modelling and coronal heating.

Other researchers have investigated the flux of magnetic helicity from active regions; here, we do the same for quiet-sun magnetic fields.

We derive a theoretical expression for the total helicity flux in terms of "mutual" and "self" helicities, which arise from the relative motions of separate flux elements and the time evolution of the quadrupole moments of individual magnetic flux elements, respectively.

Using a tracking algorithm applied to high cadence, high resolution SOHO/MDI magnetograms, we determine the observed rate of self helicity flux in the quiet sun and compare these measurements with our theoretical predictions.

Of note, we find that the orientations of small-scale flux elements in the quiet sun are not random.

0: One Minute of Solar Magnetism

'If it were not for its variable magnetic field, the Sun would have been a rather uninteresting star.' – E.N. Parker

Magnetic fields are omnipresent in the solar atmosphere, and have been grouped into TWO classes –

1. "ACTIVE REGION" fields:
   (a) SCALE: $\sim 10^{21}$ Mx (1 Mx = 1 G $\cdot$cm^2)
   (b) HISTORY: oldest known – Chinese records $\sim 10^3$ yrs. old!
   (c) SPATIAL DIST'N: $\lesssim 35°$ lat. from equator, seen to **emerge** and **diffuse** over time
   (d) TEMPORAL BEHAVIOR: come and go in 11 yr. cycle, from "solar dynamo," originate near $.7R_\odot$; generate flares, CME's
   (e) WHOLE-CYCLE FLUX: $\sim 10^{24}$ Mx
2. "QUIET SUN" fields:
   (a) SCALE: $\sim 10^{18}$ Mx
   (b) HISTORY: only really manifested spectroscopically
   (c) SPATIAL DIST'N: $\sim$ everywhere on Sun's surface! $N \sim 10^4$
   (d) TEMPORAL BEHAVIOR: come and go in ~ 40 hr
   (e) WHOLE-CYCLE FLUX: $\sim 10^{25}$ Mx, if made anew every 40 hr.

3

$\frac{1}{2}$: What is Magnetic Helicity?

- "Magnetic helicity" is commonly used to mean
$$\mathcal{H}_{M_0} \equiv \int dV(\mathbf{A}\cdot\mathbf{B}) = \int dV(\mathbf{A}\cdot(\nabla\times\mathbf{A}))\ .$$
- This integral quantifies the linkages among all pairs of field lines.
- DETAIL: If B_n on surface S bounding V does not vanish, then $\mathcal{H}_M$ does not satisfy gauge invariance – but $B_n|_S \neq 0$ on the Sun!
- This led Berger & Field (1984) to define a gauge-invariant *relative helicity*,
$$\mathcal{H}_{M_R} \equiv \int dV(\mathbf{A}+\mathbf{A_P})\cdot(\mathbf{B}-\mathbf{B_P})\ ,$$
where
  - $\mathbf{B}_P$ is the current-free field matching $B_n|_S$; } FICTITIOUS!
  - $\mathbf{A}_P$ is a vector potential for $\mathbf{B}_P$;
  - 'REAL' { $\mathbf{B}$ is the actual magnetic field; and
  - $\mathbf{A}$ is a vector potential for $\mathbf{B}$.

4

1.1: Motivation: Why do we care about helicity transport?

A. dynamo theories $\Longleftrightarrow$ helicity budget

B. if $\mathcal{H}_m$ is proxy for J, then $\mathcal{H}_M$ flux feeds energy into "magnetic carpet" $\Longrightarrow$ coronal heating implications

C. lat./long. dependences in $\mathcal{H}_M$-flux $\Longleftrightarrow$ ultimate fate of active region flux

D. possible comparison of source of helicity with w/*in situ* measurements of $\mathcal{H}_M$-flux in solar wind at 1 AU

E. "hot topic!" recent papers by Berger & Ruzmaikin (1999), DeVore (2000), Chae (2000, 2001), Demoulin *et al* (2001), study $\mathcal{H}_M$-flux in active regions

1.2 Goal: Measure Helicity Flux through Photosphere

- Why photosphere? We can measure B_z there!
- Take photosphere as $z = 0$ plane in Cartesian geometry.
- Relative helicity flux through photosphere is

$$\frac{d\mathcal{H}_{M_R}}{dt} = 2\oint_S da\Big(\underbrace{(\mathbf{A_P}\cdot\mathbf{B})v_z}_{\text{advection}} - \underbrace{(\mathbf{A_P}\cdot\mathbf{v})B_z}_{\text{"braiding"}}\Big)\,.$$

- advection term is certainly relevant for active regions; relevance for quiet-sun fluxes is less certain, so we ignore it.
- "braiding" term is actually *transport* of $\mathcal{H}_M$, not creation of helicity
- (in fact, $\mathcal{H}_m$ is well-conserved in high $\mathcal{R}_M$ plasmas, even during "fast" magnetic reconnection events!)

"Braiding" term corresponds to winding of field lines.

2. Theoretical Approach

- Assume magnetic field at surface arises from N small, isolated "point-like" sources,

$$B_z(\mathbf{x}) \sim \sum_{i=1}^{N} \Phi_i \delta(\mathbf{x} - \mathbf{x}_i) \ .$$

- In Coulomb guage, vector potential for the current-free field $\mathbf{B}_P$, evaluated on the surface, is

$$\mathbf{A}_P(\mathbf{x}) = \sum_{i=1}^{N} \frac{\Phi_i}{2\pi} \frac{\hat{z} \times (\mathbf{x} - \mathbf{x}_i)}{|(\mathbf{x} - \mathbf{x}_i)|^2} \ ,$$

so $\mathbf{A}_P^{(i)}$ of ith source is CIRCUMFERENTIAL.

SOURCES OF B_z ARE POINT-LIKE!

a) b)

a) Quiet sun magnetic fluxes are small, isolated features. b) Point source of flux situated at origin has an azimuthal vector potential.

TANGENT LINES OF A_P

7

- The helicity flux can be broken into "self" and "mutual" parts,

$$\frac{d\mathcal{H}}{dt} = -\frac{1}{\pi} \oint da' \Big[\underbrace{\sum_i \sum_{j \neq i} \Phi_i \Phi_j \delta(\mathbf{x}' - \mathbf{x}_i) \Big(\mathbf{v} \cdot \frac{\hat{z} \times (\mathbf{x}' - \mathbf{x}_j)}{|(\mathbf{x}' - \mathbf{x}_j)|^2}\Big)}_{\text{"mutual"}} + \underbrace{\sum_i \Phi_i^2 \delta(\mathbf{x}' - \mathbf{x}_i) \Big(\mathbf{v} \cdot \frac{\hat{z} \times (\mathbf{x}' - \mathbf{x}_i)}{|(\mathbf{x}' - \mathbf{x}_i)|^2}\Big)}_{\text{"self"}} \Big] \ .$$

- *Mutual helicity* flux arises from the winding of fields from distinct sources about each other – "fluxes orbiting each other."
- *Self helicity* flux arises from the winding of field lines in a source about its own axis – "a rotating flux."

TWO PLOT LINES TO FOLLOW IN THIS "TALE OF TWO HELICITIES"

8

- 2.1 The "mutual" helicity term is easily evaluated,

$$\frac{d\mathcal{H}^{MUT}}{dt} = -\frac{1}{\pi}\Phi_i\Phi_j\Omega_{ij} \ ,$$

where $\Omega_{ij} \equiv$ angular velocity of Φ_i about Φ_j.

Q: What motions contribute to $d\mathcal{H}^{(MUT)}/dt$?

A: One example is shearing from differential rotation, which partially braids field lines' footpoints.

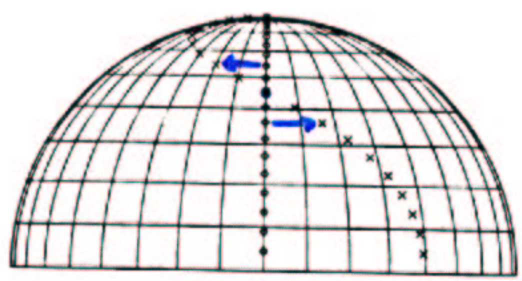

Differential rotation causes footpoints at different latitudes to wind partially around each other, as illustrated in this mapping over one mid-latitude rotation.

2.2 Self-Helicity Term

- Magnetic field doesn't *really* originate from point sources; must investigate $B_z(\mathbf{x})$ and $\mathbf{v}(\mathbf{x})$ *near* ea. flux, Φ_k.
- First, define ith coord. of flux-weighted avg. position, $\bar{\mathbf{x}}$, of kth flux, Φ_k,

$$\bar{x}_i \equiv \frac{\int_S d^2x\, B_z\, x_i}{\int_S d^2x\, B_z} = \frac{1}{\Phi_k}\int_S d^2x\, B_z\, x_i \ .$$

- Next, define local polar coordinates centered at $\bar{\mathbf{x}}$,

$$r \equiv |\delta\mathbf{x}| \equiv |\mathbf{x} - \bar{\mathbf{x}}|$$
$$\phi \equiv \sin^{-1}(\hat{z} \cdot (\hat{x} \times \delta\mathbf{x})) \ .$$

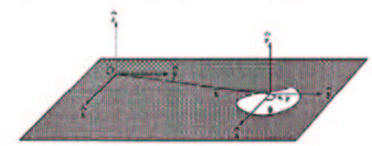

Coordinates centered at $\bar{\mathbf{x}}$, the magnetic center-of-flux.

- Now represent $B_z(r,\phi)$ near $\bar{\mathbf{x}}$ w/expansion in azimuthally orthogonal functions

$$B_z(r,\phi) = \frac{1}{2}f_0(r) + \sum_{n=2}^{\infty} f_n(r)\cos(n\phi) + g_n(r)\sin(n\phi) ,$$

- Coefficient functions $f_n(r), g_n(r)$ quantify departure of $B_z(r,\phi)$ from axisymmetry about axis through $\bar{\mathbf{x}}$.
- We define radial MOMENTS of $f_n(r)$ as

$$F_n^{(m)} \equiv \pi \int_0^{\infty} dr\, r^m f_n(r) ,$$

and similarly for $G_n^{(m)}$.

$G_2 > 0$ $F_2 > 0$ $F_2 = 0 = G_2$

a) 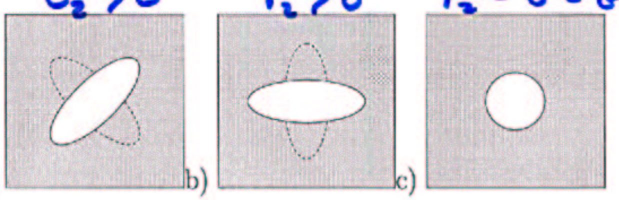 b) c)

Different flux distributions have different expansion coefficients: a) $G_2^{(m)} \neq 0$, b) $F_2^{(m)} \neq 0$, c) $F_2^{(m)} = 0 = G_2^{(m)}$.

11

- Expanding $\mathbf{v}(\mathbf{x})$ about $\bar{\mathbf{x}}$ gives

$$v_i(\delta\mathbf{x}) \simeq \bar{v}_i + \frac{\partial v_i}{\partial x_j}\Big|_{\bar{\mathbf{x}}} \delta x_j = \bar{v}_i + M_{ij}(\bar{\mathbf{x}})\delta x_j ,$$

where $\bar{v}_i$ is center-of-flux velocity in $\hat{x}_i$ direction.

- The Jacobian matrix M_{ij} can be written

$$\begin{pmatrix} M_{11} & M_{12} \\ M_{21} & M_{22} \end{pmatrix} = D\begin{pmatrix} 1 & 0 \\ 0 & 1 \end{pmatrix} + C\begin{pmatrix} 0 & -1 \\ 1 & 0 \end{pmatrix} + T\begin{pmatrix} 1 & 0 \\ 0 & -1 \end{pmatrix} + X\begin{pmatrix} 0 & 1 \\ 1 & 0 \end{pmatrix} .$$

where

$$\begin{cases} D \equiv (M_{11}+M_{22})/2 \equiv \frac{1}{2}\mathrm{Tr(M)} & (\text{"divergence"}) \\ C \equiv (M_{12}-M_{21})/2 \equiv \text{antisymmetric} & (\text{"curl"}) \\ T \equiv (M_{11}-M_{22})/2 \equiv \text{traceless,diagonal} & (\text{"+"-flow}) \\ X \equiv (M_{12}+M_{21})/2 \equiv \text{traceless,off-diagonal} & (\text{"x"-flow}) . \end{cases}$$

THESE CAN REPRESENT AN ARBITRARY FLOW.

a) 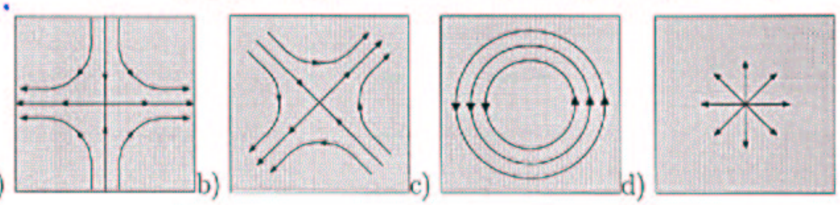 b) c) d)

"Elemental" flows that can be superposed to represent any flow field locally: a) "t" flow, b) "x" flow, c) "curl" flow, d) "diverging" flow.

12

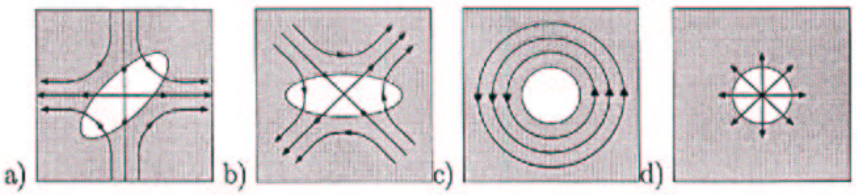

Flows "generating" helicity with particular flux distributions: a) "+" flow, b) "x" flow, c) "curl" flow. d) "Diverging" flow might signal helicity advection.

- Combining M_{ij} with $F_n^{(j)}$ and $G_n^{(j)}$ gives the first order self helicity flux,

$$\frac{d\mathcal{H}^{SELF}}{dt} = -\Phi^2\left(C + XF_2^{(1)} - TG_2^{(1)}\right) .$$

- *Q:* Can we measure C, X, and T from $B_z(\mathbf{x}, \mathbf{t})$?
- Change in flux element's shape determined by time derivs of moments of normed flux distribution,

$$\frac{d}{dt}\langle\delta x_1^2\rangle = \frac{d}{dt}\frac{1}{\Phi_0}\int_S d^2x\, B_z(x_1 - \bar{x}_1)^2 \rightarrow \frac{1}{2}\left(\frac{\Delta F_0^{(3)}}{\Delta t} + \frac{\Delta F_2^{(3)}}{\Delta t}\right)$$

$$\frac{d}{dt}\langle\delta x_2^2\rangle = \frac{d}{dt}\frac{1}{\Phi_0}\int_S d^2x\, B_z(x_2 - \bar{x}_2)^2 \rightarrow \frac{1}{2}\left(\frac{\Delta F_0^{(3)}}{\Delta t} - \frac{\Delta F_2^{(3)}}{\Delta t}\right)$$

$$\frac{d}{dt}\langle\delta x_1\,\delta x_2\rangle = \frac{d}{dt}\frac{1}{\Phi_0}\int_S d^2x\, B_z(x_1 - \bar{x}_1)(x_2 - \bar{x}_2) \rightarrow \frac{1}{2}\left(\frac{\Delta G_2^{(3)}}{\Delta t}\right) .$$

- Assuming B_z is conserved, it obeys a 2-d continuity equation,

$$\frac{\partial B_z}{\partial t} + \nabla\cdot(\mathbf{v}B_z) = 0 .$$

We can then relate the time evolution of the moments to the flow field via a "shape matrix,"

$$\frac{1}{2\Delta t}\begin{pmatrix} \Delta F_0^{(3)} + \Delta F_2^{(3)} \\ \Delta F_0^{(3)} - \Delta F_2^{(3)} \\ \Delta G_2^{(3)} \end{pmatrix} = \begin{pmatrix} (+F_0^{(3)} + F_2^{(3)}) & (G_2^{(3)}) & -(G_2^{(3)}) & (F_0^{(3)} + F_2^{(3)}) \\ (-F_0^{(3)} + F_2^{(3)}) & (G_2^{(3)}) & +(G_2^{(3)}) & (F_0^{(3)} - F_2^{(3)}) \\ 0 & (F_0^{(3)}) & (F_2^{(3)}) & (G_2^{(3)}) \end{pmatrix}\begin{pmatrix} T \\ X \\ C \\ D \end{pmatrix} .$$

- In words: THE TIME RATE OF CHANGE OF A FLUX'S SHAPE IS RELATED TO THE SHAPE OF THE FLUX AND THE FLOW THAT ADVECTS IT.
- Thus, we seek the *FOUR* unknowns T, X, C, D, given only *THREE* observables, $d(\langle\delta x_i \delta x_j\rangle)/dt$.

- Every flux distribution has some flow field which lies in null space of "shape matrix."
- These "null flows" *do*, in general, inject helicity!
- As shape of flux evolves, null space of flow field does, too – which we can use to our advantage!

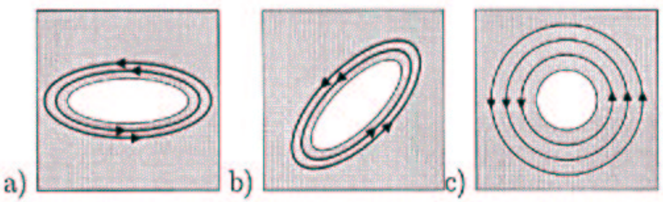

For every flux distribution, some flow field will not alter its shape.

Our method:

1. Use SVD find null space at each time step.
2. Use a relaxation algorithm to add "null flow" to minimize time derivatives of flow components.
3. Use Monte Carlo routine to estimate errors in inverted flow comps.
4. Use flow field (C, X, T) found this way to compute self helicity flux,

$$\frac{d\mathcal{H}^{SELF}}{dt} = -\Phi^2\left(C + XF_2^{(1)} - TG_2^{(1)}\right) .$$

Test: Rotate simulated flux w/ "pudgy ellipse" shape about its axis, through 2π rad, then find flow!

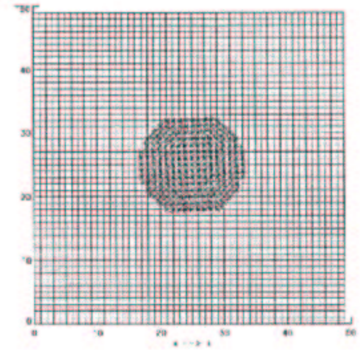

Simulated Data for Self Helicity Test

Q: How did our algorithm do at finding the known flow?

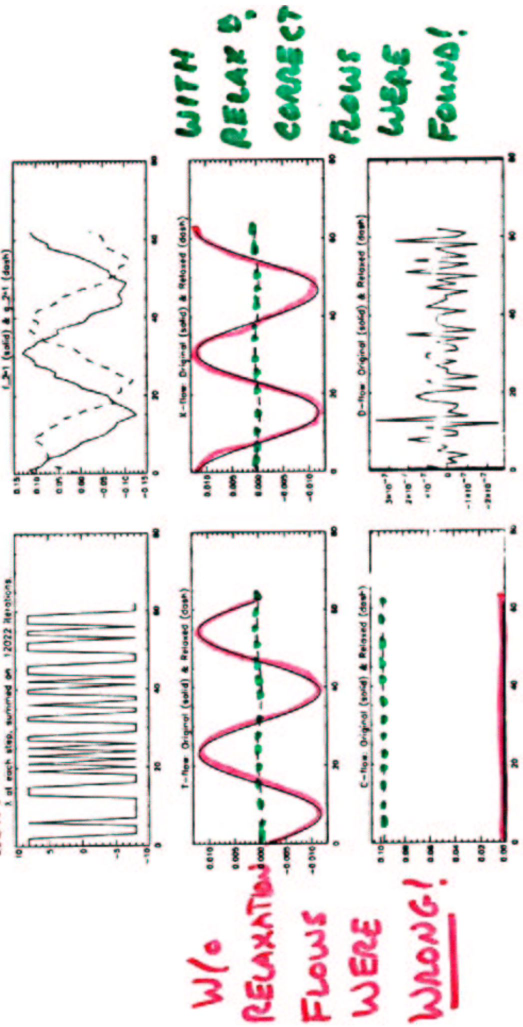

SVD and Relaxation Test Inversion, Plots

17

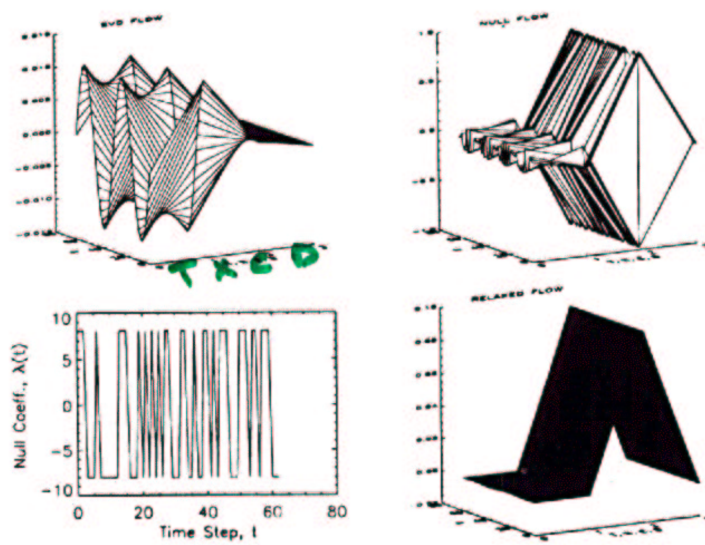

SVD and Relaxation Test Inversion, Surfaces

18

3. Methods: Helicity Flux Measurement in 3 Easy Steps!

i. label fluxes and record structural attributes

ii. track fluxes and evolution of their structure

iii. compute $\mathcal{H}$ flux!

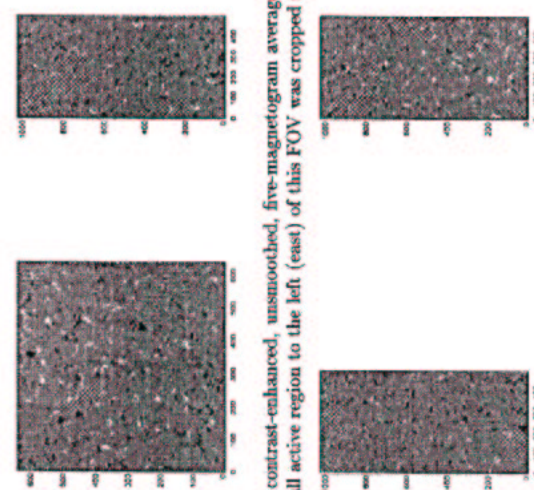

The first contrast-enhanced, unsmoothed, five-magnetogram average image from data sets # 1 and # 2a. A small active region to the left (east) of this FOV was cropped from the full image in set # 1.

The first contrast-enhanced, unsmoothed, five-magnetogram average image from data sets # 2b and # 2c.

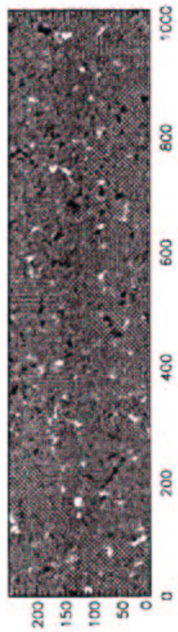

The first contrast-enhanced, unsmoothed, five-magnetogram average image from data set # 3. A small active region below this FOV was cropped from the full image.

3.1 Data & Handling

- SoHO MDI line-of-sight magnetograms, photospheric B_z found from Stokes V profile in Ni I (6768 Å) line
- "high res" mode: .61" pixels (c. 442 km)
- average 5 images taken with 1 min. cadence
- smooth on c. 3 pixels by convolution w/"potential extrapolation" kernel
- fit core with Gaussian; shift data by centroid

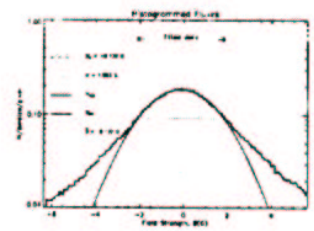

Histograms of field strengths in magnetograms from data set 1. We fit the 4 G "core" of histogram with a Gaussian. The fit is slightly displaced from zero, and we shift the data by the negative of the displacement. We take the error in field strength per pixel, σ, to be the fitted width of the Gaussian.

3.2 Labelling of Flux Elements

- use single-pass "flux-ranked uphill gradient" method to label pixels in convex groups
- c. 700 labels with (1024 x 1024) pixels & 10 G threshold
- require group size > 10 pixels (c. 500 elements in (1024 x 1024) pixels), then compute & record:
  1. total flux, Φ
  2. location magnetic center of flux, $\bar{\mathbf{x}}$
  3. flux's moments, $F_2^{(m)}, G_2^{(m)}$, etc.

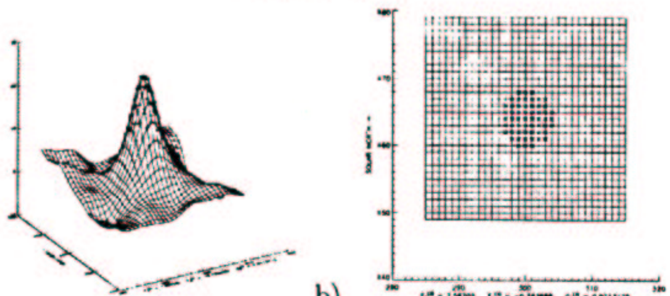

a) b)

Surface plot of magnetic field strength, in Gauss, measured by SoHO/MDI. Asterisks mark pixels grouped into one mostly-axisymmetric magnetic flux element, shown in a) perspective and b) overhead views.

Labelling Results

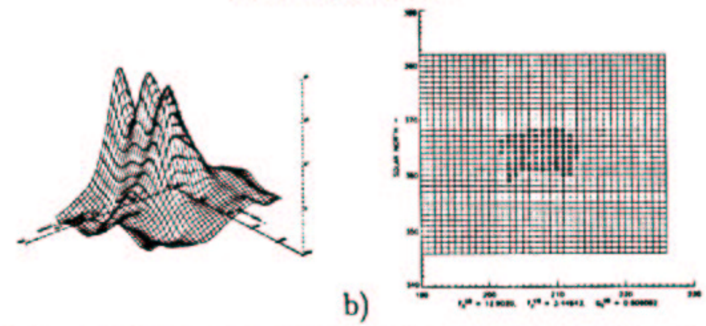

a) b)

Labelling algorithm uses convexity of measured magnetic field to group pixels into flux elements. Asterisks mark pixels grouped into one magnetic flux element, shown in a) perspective and b) overhead views.

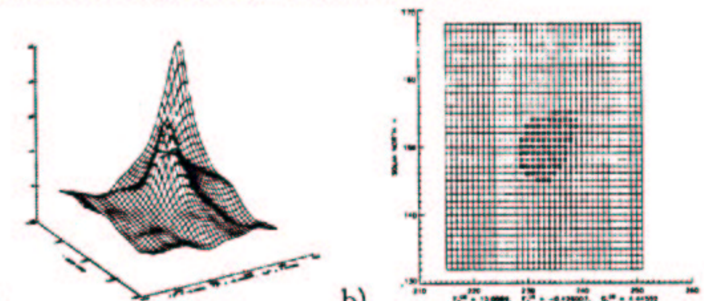

a) b)

Asterisks mark pixels grouped into one magnetic flux element, shown in a) perspective and b) overhead views.

Flux Elements' Shapes Not Random!

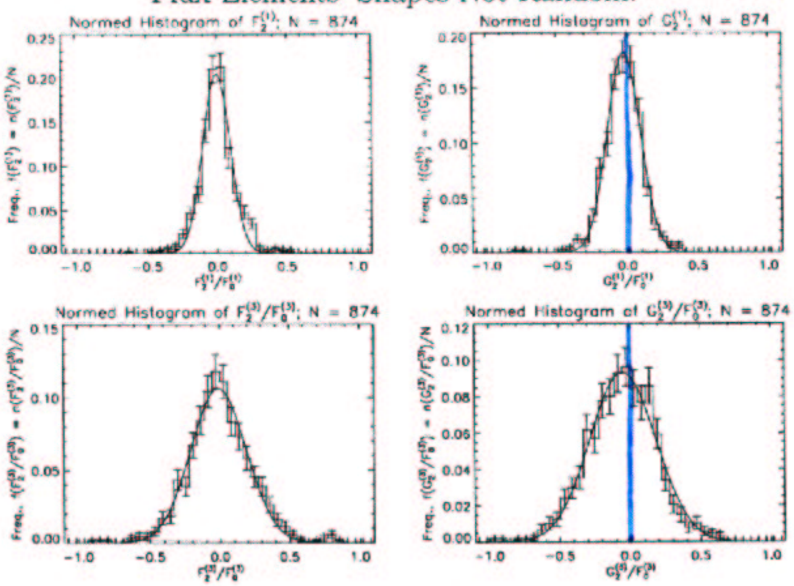

Histograms of shape coefficients $F_2^{(m)}$ and $G_2^{(m)}$, normalized to the relevant azimuthal mode, $F_0^{(m)}$: $F_2^{(1)}, G_2^{(1)}, F_2^{(3)}/F_0^{(3)}, G_2^{(3)}/F_0^{(3)}$, from data set 1.

- In *all* cases, the average, median, and fitted centroid are all to the *left* of zero.
- Asymmetries transform as expected as data are flipped. Some edge effects are present.
- Typical values from data set # 1 are $\sigma \sim .2$, with mean/median $\sim -.02$, meaning observed displacements of distributions' centroids are $\gtrsim 3\sigma/\sqrt{N}$

Tracking Results

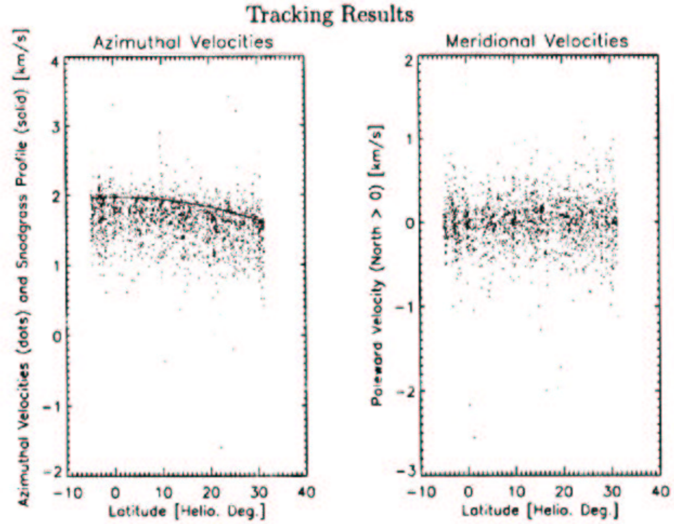

Plotted sidereal rotational (left) and meridional velocities (right), as a function of heliographic latitude in data set # 2a. The Snodgrass differential rotation profile is shown in the left plot.

- Flux elements' rotational velocities are slightly sub-differential.
- Average meridional velocities are ~ 10 m/s northward.

24

5.2. Results: Self Helicity

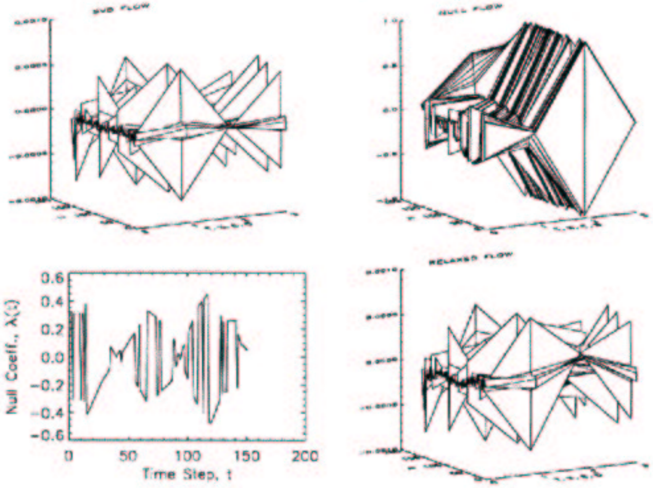

SVD/Relax'n Data Inversion: "SVD Flow", Null Space, Null Comps., "Relaxed Flow"

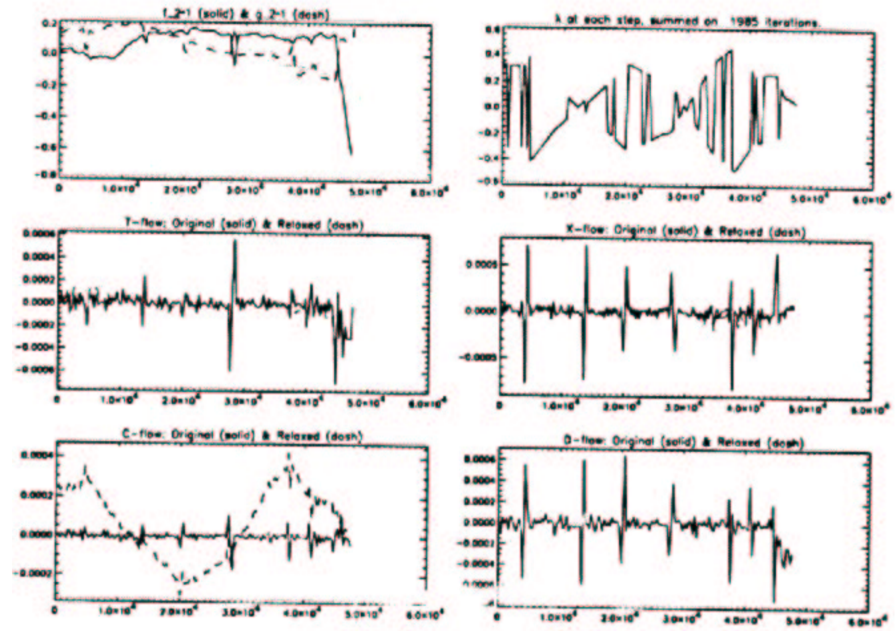

SVD/Relax'n Data Inversion: Shape Coefficients, Null Components, Inverted Flow Comps.

- Q: What gives rise to SPIKES seen in inverted flows?

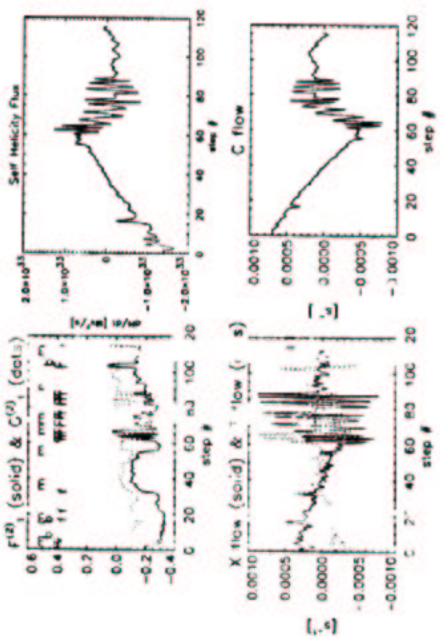

Event history and inverted flows for a flux element in data set # 2a.

- Fragmentations, collisions, and data gaps affect the time rate of change of flux elements' shapes, which can affect the inverted flows.

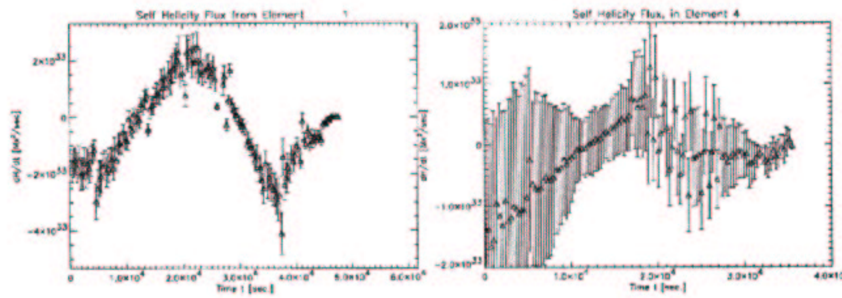

Time series of self-helicity flux for individual flux elements from data sets # 1 and # 2a, respectively.

- Sometimes error bars are large. The inversion procedure is not the most robust!
- Fluctuations take place on long time scales. A result of the relaxation algorithm?

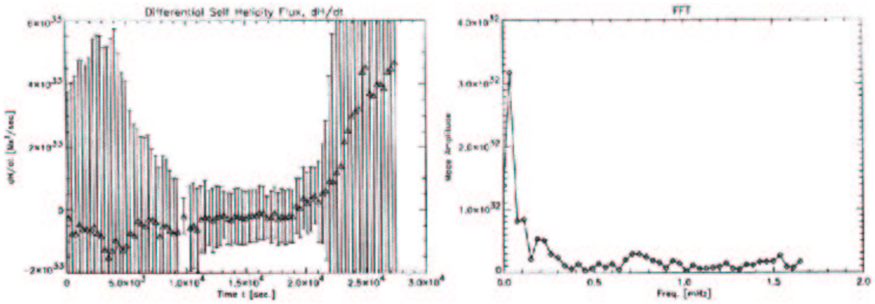

Time series of self-helicity flux for ALL flux elements from data set # 3, and its Fourier transform.

- Error bars can be very large!
- Avg. $d\mathcal{H}^{(SELF)}/dt$ varied in sign in different data sets, and is small (~ .1%) compared to ~ $10^{33}\mathrm{Mx}^2/\mathrm{s}$ fluctuations.
- Long-time-scale fluctuations still present. "Collective behavior," or superposition of artifacts of many relaxation results?
- Fluctuations are consistent with measurement errors about a mean self-helicity flux equal to either zero or average measured value.

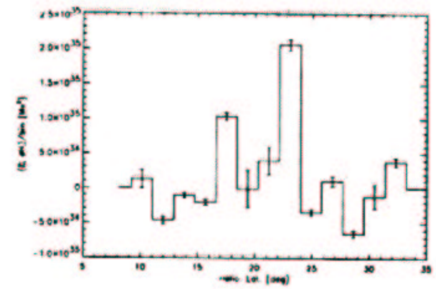

The flux of self-helicity, binned by magnetic flux element latitude.

- The flux of self-helicity shows no dependence on flux element latitude.
- Shear from differential rotation acting on individual fluxes would presumeably introduce such a dependence.
- From these data, we infer no such shear operates on the small spatial scales of individual fluxes.

Mutual Helicity Fluxes

Data Set #	$\langle d\mathcal{H}/dt\rangle_t \pm s$	$\langle d\mathcal{H}/dt\rangle_\sigma \pm \bar{\sigma}$	median($d\mathcal{H}_i/dt$)	$\langle d\mathcal{H}/dt\rangle_{pp} \pm \sigma_{pp}$
1	$-.443 \pm 80.63$	$-.0187 \pm 4.29$	-6.85	$-.00457 \pm 1.05$
2a	-10.2 ± 328	-3.26 ± 5.34	6.39	$-.637 \pm 1.04$
2b	-41.7 ± 313	-16.1 ± 4.79	-2.75	$-3.14 \pm .936$
2c	-93.5 ± 590	-116 ± 13.5	-86.2	-22.7 ± 2.64
3	-9.78 ± 48.0	-5.92 ± 1.99	-6.09	$-2.31 \pm .777$

$\times 10^{33}$ $\times 10^{33}$ $\times 10^{33}$ $\times 10^{28}$

Self Helicity Fluxes

Set #	$\langle N\rangle_t$	$\langle d\mathcal{H}_i/dt\rangle_t \pm s$	$\langle d\mathcal{H}_i/dt\rangle_\sigma \pm \sigma$	median($d\mathcal{H}_i/dt$)	$\langle d\mathcal{H}/dt\rangle_{pp} \pm \bar{\sigma}_{pp}$
1	194	$.311 \pm 1.17$	5.35 ± 2.75	5.15	2.54 ± 13.04
2a	246	$-.0322 \pm 1.21$	2.46 ± 2.10	-8.68	11.8 ± 10.1
2b	256	$.0225 \pm 2.42$	-17.2 ± 1.78	-15.9	-86.0 ± 8.96
2c	271	$-.187 \pm 7.75$	-1.87 ± 2.18	-7.15	-9.89 ± 11.54
3	113	$.0333 \pm 1.14$	13.1 ± 5.32	41.5	57.6 ± 23.5

$\times 10^{32}$ $\times 10^{27}$ $\times 10^{27}$ $\times 10^{23}$

∞.1 Conclusions

- Average self-helicity flux was $\sim 10^{28}$ Mx^2/s, while fluctuations were $\sim 10^{33}$ Mx^2/s.
- Prediction for self-helicity flux based upon shear from differential rotation was $\sim 10^{33}$ Mx^2/s, much higher than observed self helicity flux. But self-helicity flux exhibits no differential-rotation-like latitudinal dependence!
- Of note: flux element shapes are not random!
- (FYI: Observed mutual helicity flux was much greater [$\times 10^4$] than self helicity flux, as predicted.)

∞.2 Future Directions

- Might want to characterize helicity transport vs. time in solar cycle.
- Want to apply these techniques to active regions' evolution.
- Might try to characterize flow field vs. lat./long., time in cycle, etc., while doing so.